

UFO: Unlocking Ultra-Efficient Quantized Private Inference with Protocol and Algorithm Co-Optimization

Wenxuan Zeng¹², Chao Yang¹², Tianshi Xu¹³, Bo Zhang⁴, Changrui Ren⁴, Jin Dong⁴, Meng Li^{13†}

¹Institute for Artificial Intelligence, Peking University, China

²School of Software and Microelectronics, Peking University, China

³School of Integrated Circuits, Peking University, China

⁴Beijing Academy of Blockchain and Edge Computing

Abstract—Private convolutional neural network (CNN) inference based on secure two-party computation (2PC) suffers from high communication and latency overhead, especially from convolution layers. In this paper, we propose UFO, a quantized 2PC inference framework that jointly optimizes the 2PC protocols and quantization algorithm. UFO features a novel 2PC protocol that systematically combines the efficient Winograd convolution algorithm with quantization to improve inference efficiency. However, we observe that naively combining quantization and Winograd convolution faces the following challenges: 1) *From the inference perspective*, Winograd transformations introduce extensive additions and require frequent bit width conversions to avoid inference overflow, leading to non-negligible communication overhead; 2) *From the training perspective*, Winograd transformations introduce weight outliers that make quantization-aware training (QAT) difficult, resulting in inferior model accuracy. To address these challenges, we co-optimize both protocol and algorithm. 1) *At the protocol level*, we propose a series of graph-level optimizations for 2PC inference to minimize the communication. 2) *At the algorithm level*, we develop a mixed-precision QAT algorithm based on layer sensitivity to optimize model accuracy given communication constraints. To accommodate the outliers, we further introduce a 2PC-friendly bit re-weighting algorithm to increase the representation range without explicitly increasing bit widths. With extensive experiments, UFO demonstrates 11.7×, 3.6×, and 6.3× communication reduction with 1.29%, 1.16%, and 1.29% higher accuracy compared to state-of-the-art frameworks SiRNN, COINN, and CoPriv, respectively.

I. INTRODUCTION

Private deep neural network (DNN) inference based on secure two-party computation (2PC) provides cryptographically strong data privacy protection [1]–[7]. 2PC inference frameworks target protecting the privacy of both model parameters held by the server and input data held by the client. By jointly executing a series of 2PC protocols, the client can learn the final inference results but nothing else on the model can be derived from the results. Meanwhile, the server knows nothing about the client’s input [1]–[6], [8]–[10].

However, 2PC frameworks achieve high privacy protection at the cost of orders of magnitude latency and communication overhead due to the massive interaction between the server and client. As shown in Figure 1(a) and (b), the total communication of a convolutional neural network (CNN) is dominated by its convolution layers while the online communication is generated by non-linear functions, e.g.,

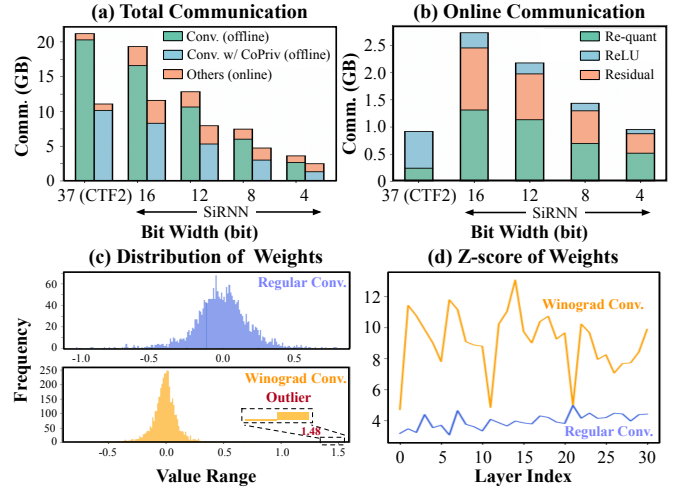


Fig. 1: Motivating inspirations. (a) Total communication and (b) online communication breakdown on the ResNet-50 block profiled with CryptFlow2 (CTF2) [1] (uniform 37-bit) and SiRNN [2] (low precision); (c) weight distributions in regular and Winograd convolution; (d) z-score (defined as the ratio between max-average and standard deviation) indicates weight outliers consistently exist after Winograd transformation across different layers.

ReLU. To improve communication efficiency, a series of works have proposed algorithm and protocol optimizations [2], [6], [11]–[13]. Typically, CoPriv [11] proposes a Winograd-based convolution protocol to reduce the communication-expensive multiplications at the cost of more local additions. Although it achieves 2× communication reduction, it still requires more than 2GB of communication for a single ResNet-18 block. Recent works also leverage mixed-precision quantization for communication reduction [2], [6], [13]. Although total communication reduces consistently with the inference bit widths, as shown in Figure 1(b), existing mixed-precision protocols suffer from much higher online communication even for 4 bits due to complex protocols like re-quantization and residual.

As the communication of 2PC frameworks scales with both the inference bit widths and the number of multiplications, we propose to combine the Winograd convolution with low-precision quantization. However, we observe a naive combination leads to limited improvement. On one hand,

† Corresponding author: meng.li@pku.edu.cn

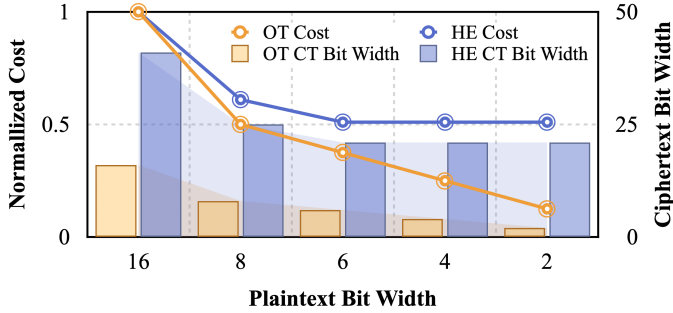


Fig. 2: Comparison between OT and HE with quantization. HE requires much higher ciphertext (CT) bit widths and cannot utilize low precision, e.g., 4 bits.

although the local additions in the Winograd transformations do not introduce communication directly, they require higher inference bit widths to avoid inference overflow and complicate the bit width conversion protocols. As a result, a naive combination only reduces $\sim 20\%$ total communication with even more online communication compared to not using Winograd convolution as shown in Figure 1(a). On the other hand, the Winograd transformations also distort the model weight distribution such that introduce more outliers that make quantization harder, as shown in Figure 1(c) and (d). Hence, training a quantized model with outliers inevitably results in inferior model accuracy.

In this paper, we propose an efficient 2PC framework named UFO to solve the aforementioned challenges. UFO systematically combines Winograd convolution with quantization and features a series of protocol and algorithm optimizations. Our contributions can be summarized below:

- **At the protocol level.** We observe the communication of 2PC inference scales with both the bit widths and the number of multiplications. Hence, we propose UFO, a novel convolution protocol that systematically combines Winograd convolution and mixed-precision quantization for efficient inference. UFO features a series of graph-level optimizations to reduce online communication.
- **At the algorithm level.** We propose a 2PC-aware mixed-precision Winograd quantization-aware training (QAT) algorithm and further develop a 2PC-friendly bit re-weighting algorithm to handle the outliers introduced by the Winograd transformations and improve the accuracy.

Evaluation results. Extensive experiments demonstrate that UFO achieves $11.7\times$, $3.6\times$, and $6.3\times$ communication reduction with 1.29%, 1.16%, and 1.29% higher accuracy compared to state-of-the-art frameworks SiRNN, COINN, and CoPriv, respectively.

II. PRELIMINARIES AND BACKGROUNDS

A. Threat Model

UFO is a 2PC-based private inference framework that involves a client and a server. The server holds the private model weights and the client holds the private input data. Following [1]–[4], [8], [14], [15], we assume the DNN architecture (including the number of layers and the operator type, shape,

and bit widths) are known by two parties. At the end of the protocol execution, the client learns the inference result and the two parties know nothing else about each other’s input. Consistent with prior works, UFO adopts a *honest-but-curious* security model¹ where both parties follow the protocol specifications but also attempt to learn more from the information than allowed. We also assume no trusted third party exists [1], [2], [4]. We also elaborate on the security and correctness analysis of UFO in Section IV-D. For clarity, we summarize the protocols used in this paper in Table I and notations in Table II.

B. Private Inference

Existing 2PC inference can be divided into OT-based and homomorphic encryption (HE)-based. HE-based methods [16]–[26] use HE to compute linear layers with lower communication compared to OT-based methods at the cost of more computation for both the server and client. Hence, they have different applicable scenarios [11], [13], [27].

In this paper, we focus on OT-based methods instead of HE-based methods. On the one hand, HE usually requires the client to have a high computing capability for encryption and decryption. On the other hand, HE is not friendly to quantization. As shown in Figure 2, there are two main reasons: 1) HE requires significantly higher ciphertext bit widths to ensure decryption correctness [28]; 2) HE cannot utilize low-precision quantization (e.g., 4-bit) because suitable prime moduli are unavailable at such low bit widths [29].

We leave detailed related work in Section VII, and we compare UFO with previous works qualitatively in Table III. UFO jointly optimizes both protocol and algorithm to simultaneously reduce the number of multiplication and communication per multiplication for efficient 2PC inference.

C. Secret Sharing and OT-based Linear Layer

Figure 4 demonstrates the protocol of 2PC inference based on OT [1], [4], [30]. With arithmetic secret sharing, each intermediate activation tensor in the i -th layer, e.g., x_i , is additively shared where the server holds $\langle x_i \rangle_s$ and the client holds $\langle x_i \rangle_c$ such that $x_i = \langle x_i \rangle_s + \langle x_i \rangle_c$ [3]. To generate the result y_i of a linear layer, e.g., general matrix multiplication (GEMM), the server and client jointly execute computation at the pre-processing (offline) stage and online stage [4]. In the pre-processing stage, the client and server first sample random r_i and s_i , respectively. Then, $\langle y_i \rangle_c = w_i \cdot r_i - s_i$ can be computed with a single OT if $r_i \in \{0, 1\}$ for 1 bit. When w_i has l_w bits, we can repeat the OT protocol l_w times by computing $w_i^{(b)} \cdot r_i - s_i$ each time, where $w_i^{(b)}$ denotes the b -th bit of w_i . The final results can then be acquired by shifting and adding the partial results together. Compared with the pre-processing stage, the online stage only requires very little communication to obtain $\langle y_i \rangle_s = w_i \cdot (x_i - r_i) + s_i$.

¹Malicious security model is also an important research direction but is not the focus of this paper.

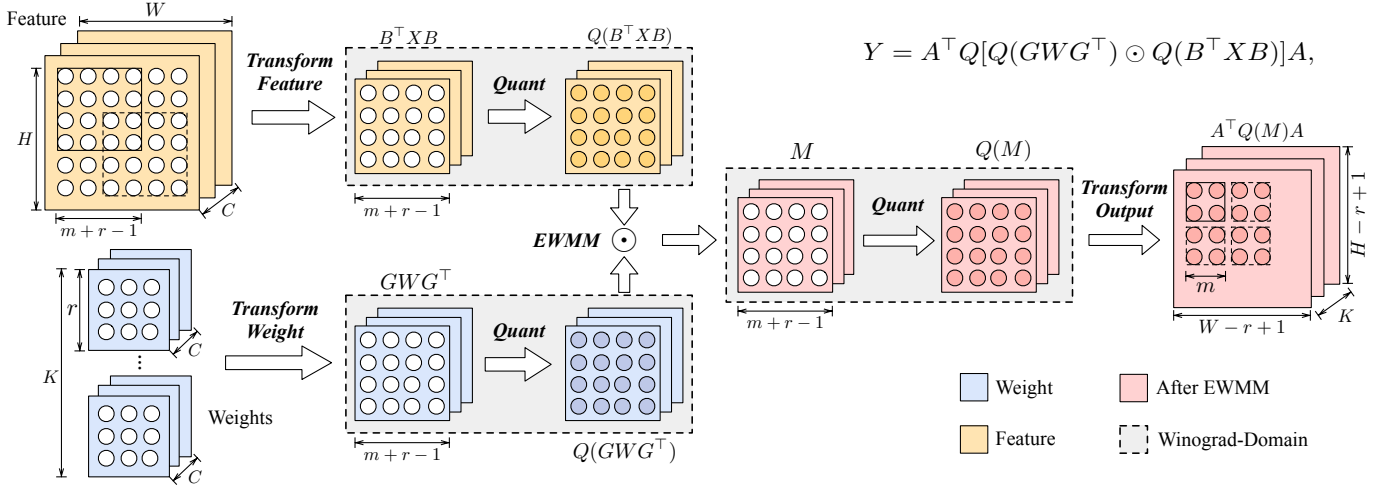


Fig. 3: Overall pipeline of Winograd convolution with low-precision quantization.

TABLE I: Underlying protocols used in this paper.

Underlying Protocol	Description	Communication Complexity
$\langle z \rangle^{(l_2)} = \Pi_{\text{Ext}}^{l_1, l_2}(\langle x \rangle^{(l_1)})$	Extend l_1 -bit x to l_2 -bit z such that $z^{(l_2)} = x^{(l_1)}$	$O(\lambda(l_1 + 1) + 13l_1 + l_2)$
$\langle z \rangle^{(l_1)} = \Pi_{\text{Trunc}}^{l_1, l_2}(\langle x \rangle^{(l_1)})$	Truncate (right shift) l_1 -bit x by l_2 -bit such that $z^{(l_1)} = x^{(l_1)} \gg l_2$	$O(\lambda(l_1 + 3) + 15l_1 + l_2 + 20)$
$\langle z \rangle^{(l_1 - l_2)} = \Pi_{\text{TR}}^{l_1, l_2}(\langle x \rangle^{(l_1)})$	Truncate l_1 -bit x by l_2 -bit and discard the high l_2 -bit such that $z^{(l_1 - l_2)} = x^{(l_1)} \gg l_2$	$O(\lambda(l_2 + 1) + 13l_2 + l_1)$
$\langle z \rangle^{(l_2)} = \Pi_{\text{Requant}}^{l_1, s_1, l_2, s_2}(\langle x \rangle^{(l_1)})$	Re-quantize x with l_1 -bit and s_1 scale to z with l_2 -bit and s_2 scale	Combination of $\Pi_{\text{Ext}}, \Pi_{\text{Trunc}}, \Pi_{\text{TR}}$

TABLE II: Notations used in this paper.

Notation	Description
λ	Security parameter that measures the attack hardness
$l_w, l_a, l_{acc}, l_{res}, l_{add}$	Bit width of weight, activation, accumulation, residual, and addition
l_{ft_ext}, l_{out_ext}	Bit width of feature and output transformation after bit extension
$s_a, s_{acc}, s_{res}, s_{add}$	Scale of activation, accumulation, residual, and addition
$x^{(l)}, \langle x \rangle^{(l)}$	l -bit integer x and l -bit secret share
A, B, G	Winograd transformation matrices
$W_l w, A_l a$	l_w -bit weight and l_a -bit activation

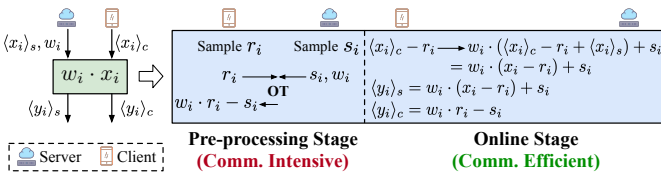


Fig. 4: Protocol of OT-based linear layer, including a pre-processing stage and an online stage to process client's input.

D. Model Quantization

Quantization converts a floating-point number into integers for better training and inference efficiency [31]–[33], which is particularly beneficial for deployment on resource-constrained devices. Specifically, a floating point number x_f can be approximated by an l_x -bit integer x_q and a scale s_x through quantization as x_q/s_x , where

$$x_q = \max(-2^{l_x-1}, \min(2^{l_x-1} - 1, \text{round}(s_x x_f))).$$

The multiplication of two floating point numbers x_f and w_f , denoted as y_f , can be approximately computed as $x_q w_q / (s_w s_x)$, which is a quantized number with $(l_x + l_w)$ -bit

and $s_w s_x$ scale. Then, y_f usually needs to be re-quantized to y_q with l_y -bit and s_y scale as follows:

$$y_q = \max(-2^{b_y-1}, \min(2^{b_y-1} - 1, \text{round}(\frac{s_y}{s_w s_x} w_q x_q))).$$

For the addition, e.g., residual connection of two quantized numbers x_q and y_q , directly adding them together leads to incorrect results. Instead, the scales and the bit widths of x_q and y_q need to be aligned first.

E. Winograd Convolution

Winograd convolution [34] is an efficient convolution algorithm that minimizes the number of multiplications. Winograd convolution can be formulated as

$$Y = W \otimes X = A^T [(GWG^T) \odot (B^T X B)]A, \quad (1)$$

where \otimes denotes regular convolution and \odot denotes element-wise matrix multiplication (EWMM). The overall pipeline is illustrated in Figure 3, and we also show where to insert the quantization operation in Winograd convolution. We follow [11] to convert EWMM into GEMM with batch optimization. A , B , and G are constant transformation matrices that are independent of the W and X and can be pre-computed based on the size of the convolution kernel and output tile m and r [34]. Weight transformation GWG^T is performed offline while feature transformation $B^T X B$ and output transformation $A^T [\cdot] A$ are performed online. The number of multiplications can be reduced from $m^2 r^2$ to $(m+r-1)^2$ at the cost of many more additions introduced by the feature and output transformation. **For 2PC inference, since transformation matrices are constant and public, $B^T X B$ and $A^T [\cdot] A$ can be computed**

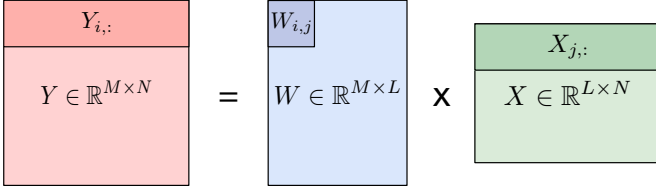


Fig. 5: An illustration of GEMM $Y = WX$.

locally without any communication. However, Winograd-domain GEMM incurs 2PC communication costs.

Considering the potential of quantization, some works combine Winograd and quantization [35]–[39]; however, they are not tailored for 2PC, resulting in suboptimal performance.

III. MOTIVATIONS

In this section, we first theoretically analyze the communication complexity of the OT-based linear layer, and then highlight the key challenges when combining Winograd convolution with quantization, which motivates UFO.

1) **Motivation 1: the total communication of OT-based 2PC inference is determined by both the bit widths and the number of multiplications in linear layers:** Consider $Y = WX$, where $W \in \mathbb{R}^{M \times L}$, $X \in \mathbb{R}^{L \times N}$ and $Y \in \mathbb{R}^{M \times N}$. With one round of OT, we can compute $W_{i,j}^{(b)} \cdot X_{j,:}$ for the b -th bit of $W_{i,j}$ and j -th row of X . Then, the i -th row of Y , denoted as $Y_{i,:}$, can be computed as

$$Y_{i,:} = \sum_{j=0}^{L-1} \sum_{b=0}^{l_w-1} 2^b \cdot W_{i,j}^{(b)} \cdot X_{j,:},$$

where l_w denotes the bit width of W . Hence, to compute $Y_{i,:}$, in total $O(l_w L)$ OTs are invoked. In each OT, the communication scales proportionally with the vector length of $X_{j,:}$, i.e., $O(N l_x)$, where l_x denotes the bit width of X . The total communication of the GEMM thus becomes $O(MLN l_w l_x)$. Hence, we observe the total communication of a GEMM scales with both the operands' bit widths, i.e., l_x and l_w , and the number of multiplications, i.e., MLN , both of which impact the round of OTs and the communication per OT. Convolutions follow a similar relation as GEMM. Hence, combining Winograd convolution and quantization is a promising solution to improve the communication efficiency of convolution layers. For non-linear layers, e.g., ReLU, communication scales proportionally with activation bit widths [2].

2) **Motivation 2: a naive combination of Winograd convolution and quantization provides limited communication reduction for 2PC inference (induced by feature and output transformation):** Although Winograd convolution reduces the number of multiplications, it is not friendly to quantized inference since it introduces many more local additions during the feature and output transformation. Hence, to guarantee the computation correctness with avoiding overflow, extra bit width conversion protocols are required as shown in Figure 6. Take ResNet-32 with 2-bit weight and 6-bit activation (W2A6) as an example in Figure 7, naively combining Winograd convolution and quantization achieves only $\sim 20\%$ communication reduction compared to not using Winograd convolution

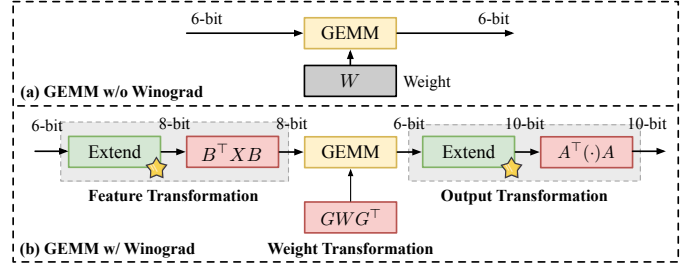


Fig. 6: Bit width conversions, i.e., extension (yellow stars) are required to avoid inference overflow during Winograd transformations with quantized 2PC inference. There is a re-quantization in GEMM to output 6-bit activation.

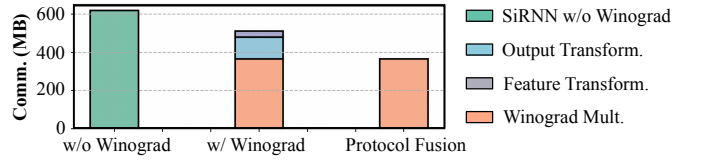


Fig. 7: Communication breakdown on ResNet-32. After protocol fusion (introduced in Section IV-B1), the communication of both feature and output transformation are totally removed.

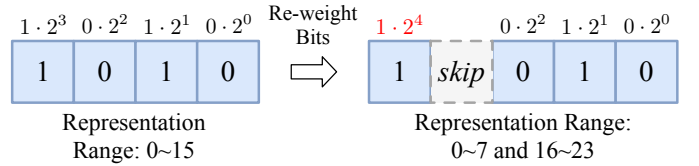


Fig. 8: Example of bit re-weighting with adjusted representation range.

in SiRNN [2], which is far less compared to the benefit of Winograd convolution [11]. Therefore, further protocol optimization is crucial to reduce the overhead induced by the bit width conversions.

3) **Motivation 3: Winograd transformations introduce weight outliers and make low-precision QAT difficult (induced by weight transformation):** Since the weight transformation involves multiplying or dividing large plaintext integers [34] and tends to generate large weight outliers, it makes the quantization challenging. Specifically, large outliers dominate the maximum magnitude measurement, leading to large quantization errors and inferior model accuracy. We show the weight distributions and z-scores with and without Winograd transformations in Figure 1(c) and (d). Instead of simply increasing the quantization bit width like previous works, we observe that it is possible to accommodate the weight outliers without explicitly increasing the bit width. Since each weight is written as $\sum_{b=0}^{l_w-1} w^{(b)} \cdot 2^b$ in OT-based linear layers, we can re-weight each bit by adjusting 2^b to increase the representation range without causing extra communication overhead. In Figure 8, bit re-weighting increases the representation range with the same bit width (note the total number of possible represented values remains the same).

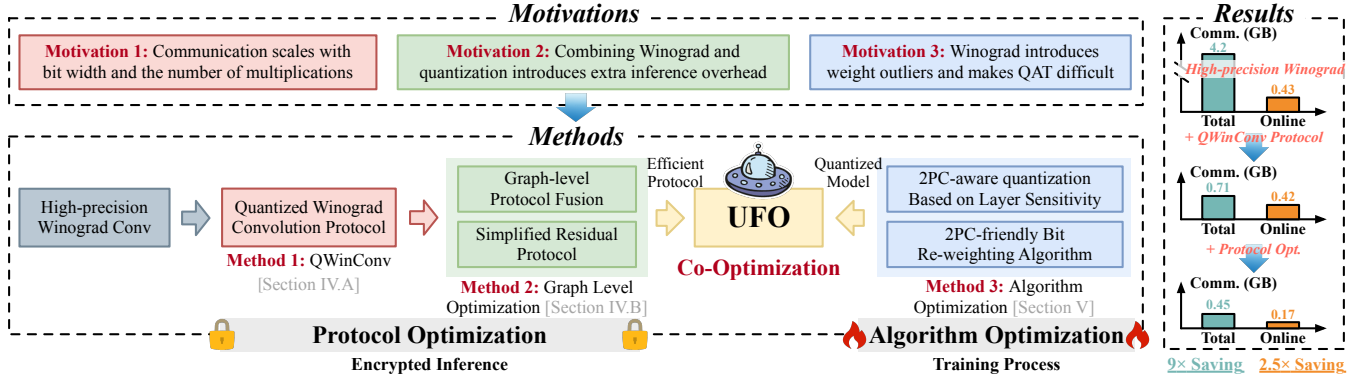


Fig. 9: Motivations and our methods of UFO. Example result is evaluated on ResNet-32 with W2A6, eventually achieving $9\times$ and $2.5\times$ total and online communication reduction.

TABLE III: Comparison with existing works. “✓” means this term can be optimized. # MUL means the number of multiplications, CPM means communication per MUL, and MP means mixed precision.

Representative Method	Protocol Optimization		Algorithm Optimization	Linear Optimization		Non-linear Optimization
	Operator Level	Graph Level		# MUL ↓	CPM ↓	
SNL [14], SENet [15], DeepReduce [8]	-	-	ReLU Pruning	-	-	✓
SiRNN [2]	Uniform Quant	MSB Opt	-	-	✓	✓
XONN [12]	Binary Quant	-	Binary Quant (Large Accuracy Drop)	-	✓	✓
ABNN2 [6]	-	-	Uniform Quant	-	✓	✓
CoPriv [11]	Winograd Conv	-	Re-param	✓	-	✓
Quotient [40]	-	-	Gradient Quant	-	✓	✓
UFO (ours)	MP Quant Winograd Conv	Simplified Residual, Protocol Fusion, MSB Opt	2PC-aware Quant, MP Quant, Bit Re-weighting	✓	✓	✓

4) **Paper Organization:** Based on the motivations, we propose UFO, a protocol-algorithm co-optimization framework for efficient 2PC inference. We show the overview in Figure 9. We first build a novel convolution protocol that combines quantization and Winograd convolution (Section IV-A). We then propose a series of graph-level optimizations, including protocol fusion to reduce the communication for Winograd transformations (Section IV-B1), simplified residual protocol to remove redundant bit width conversion protocols (Section IV-B1), and protocol optimization given known most significant bits (MSBs) (Section IV-B3). We propose a 2PC-aware mixed-precision QAT algorithm and bit re-weighting algorithm to enhance the model accuracy (Section V). We show a case evaluated on ResNet-32 with W2A6, eventually achieving $9\times$ and $2.5\times$ total and online communication reduction.

IV. INFERENCE PROTOCOL OPTIMIZATION

A. New Protocol: Quantized Winograd Convolution

As explained in Section III, when combining the Winograd convolution and quantization, extra bit extensions are needed to strictly guarantee output correctness due to local additions in the feature and output transformations.

1) **Protocol Framework:** We carefully design a 2PC framework with the quantized Winograd convolution protocol named QWinConv in Figure 10. In Figure 10(a), before QWinConv, following SiRNN [2], activations are first re-quantized to l_a -bit to reduce the communication of QWinConv (①). After QWinConv, the residual and QWinConv output are added together with the residual protocol. Residuals are

always kept in high bit width, i.e., 8-bit, for better accuracy [41]. The detailed design of QWinConv is shown in Figure 10(b), which involves 4 steps: feature transformation, weight transformation, Winograd-domain GEMM, and output transformation. We insert the bit extension protocols right before the feature and output transformation to avoid inference overflow as marked with ② and ⑤. The GEMM protocol in Figure 10(c) follows SiRNN [2] and the bit extension (③) ensures accumulation correctness. Note that weight transformation and its quantization are conducted offline, while feature transformation and output transformation are executed online.

2) **Approximation of Extension Bits and Tile Size Selection:** A natural question is “how many bits to extend for Winograd transformations while ensuring the inference correctness?” Since transformation matrices are constant and related to the tile size, we have the following lemma that bounds the outputs after transformation.

Lemma 1: Consider $Y = XB$ in feature transformation, where B is the transformation matrix. For each element $Y_{i,j}$, its magnitude can always be bounded by

$$\begin{aligned}
 |Y_{i,j}| &= \left| \sum_k X_{i,k} B_{k,j} \right| \leq \sum_k |X_{i,k}| |B_{k,j}| \\
 &\leq 2^{l_x} \sum_k |B_{k,j}| \leq 2^{l_x + \lceil \log_2 \|B_{:,j}\|_1 \rceil},
 \end{aligned}$$

where $\|\cdot\|_1$ is the ℓ_1 -norm, $\lceil \cdot \rceil$ is the ceiling operation.

Therefore, each output element $Y_{i,j}$ requires at most $l_x + \lceil \log_2 \|B_{:,j}\|_1 \rceil$ bits. Since we use per-tensor activation quantization, to strictly guarantee output correctness, we need $\lceil \max_j l_x + \log_2 \|B_{:,j}\|_1 \rceil$ bits to represent the output. Hence,

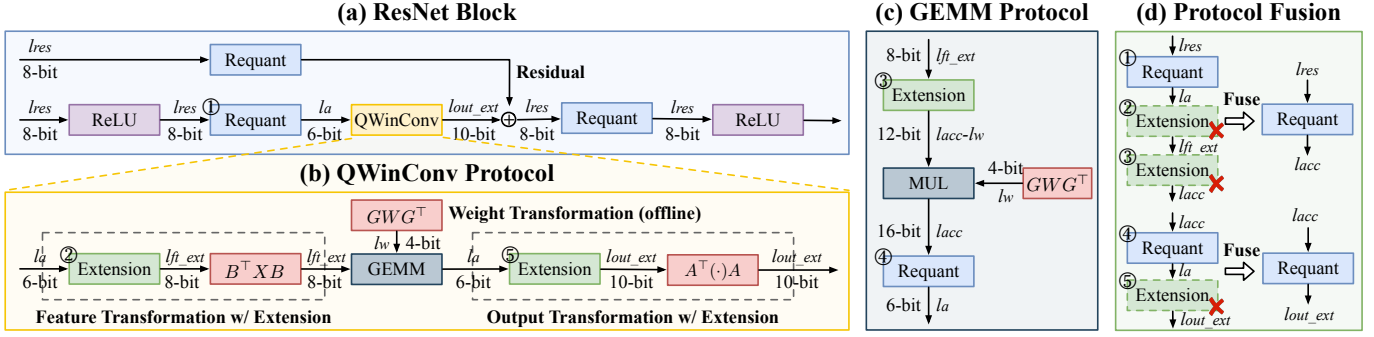


Fig. 10: Overall protocol framework with our proposed quantized Winograd convolution. l denotes the bit width and we give an example of W4A6.

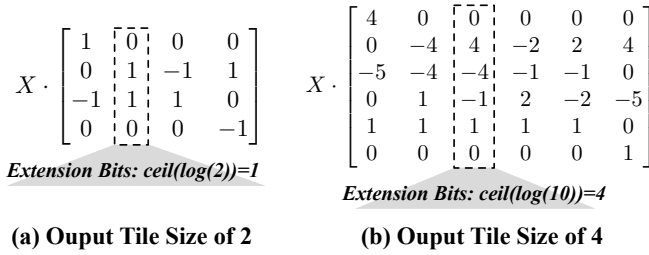


Fig. 11: XB in feature transformation. Dash boxes are the possible columns with the maximum number of additions. As a result, 2-bit and 8-bit extensions are needed for $B^T X B$.

$2 \cdot \lceil \max_j \log_2 \|B_{:,j}\|_1 \rceil$ bits are required to extend for $B^T X B$. In Figure 11, we show the transformation matrix B with the output tile size of 2 and 4. As can be calculated, 2-bit and 8-bit extensions are needed for $B^T X B$, respectively. As 8-bit extension drastically increases the communication of the following GEMM, we choose 2 as the output tile size. Output transformation can be calculated similarly and 4-bit extension is needed for $A^T[\cdot]A$ with the output tile size of 2.

Based on the above analysis, we propose the quantized Winograd convolution protocol, dubbed QWinConv, in Figure 10. Consider an example of 4-bit weights and 6-bit activations. In Figure 10(a), before QWinConv, following SiRNN [2], activations are first re-quantized to 6-bit to reduce the communication of QWinConv (block ①). We always keep the residual in higher bit width, i.e., 8-bit, for better accuracy [41], [42]. After QWinConv, the residual and QWinConv output are added together with the residual protocol. The design of QWinConv is shown in Figure 10(b), which involves four steps: feature transformation, weight transformation, Winograd-domain GEMM, and output transformation. The GEMM protocol in Figure 10(c) follows SiRNN [2] and the extension (block ③) ensures accumulation correctness. Weight transformation and its quantization can be conducted offline, while feature and output transformation and quantization must be executed online. We insert bit extensions right before the feature and output transformation (block ② and ④).

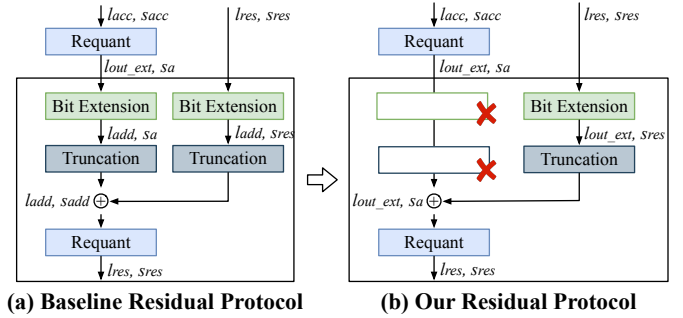


Fig. 12: Comparison between (a) baseline residual protocol [2] and (b) our simplified residual protocol. l, s mean the bit width and scale of the operand. Our protocol removes redundant bit width conversion in the main branch.

B. Graph-level Protocol Optimization

1) **Graph-level Protocol Fusion:** As explained in Section III, extra bit width conversion protocols in QWinConv increase the online communication and diminish the benefits of combining quantization with Winograd convolution, especially for low bit widths, e.g., 4-bit. We observe there are neighboring bit width conversion protocols that can be fused to reduce the overhead in Figure 10 (more details in Section IV-C). Specifically, we find two patterns that appear frequently: 1) consecutive bit width conversions, e.g., ①②, ④⑤; 2) bit width conversions that are only separated by local operations, e.g., ②③. As the cost of bit width conversion protocols is only determined by the bit width of inputs [2] as shown in Table I, such protocol fusion enables complete removal of the cost of ②③⑤ as shown in Figure 10(d), enabling efficient combination of Winograd convolution and quantization.

2) **Simplified Residual Protocol:** As shown in Figure 1(b), residual protocol consumes around 50% of the online communication due to the complex alignment of both bit widths and scales as shown in Figure 12(a). Therefore, we propose a new simplified residual protocol to reduce the communication as shown in Figure 12(b). Specifically, we directly align the bit width and scale of residual to the QWinConv output for addition. In this way, we get rid of the redundant bit width conversion protocols for the QWinConv output. As demonstrated in Section VI-B, UFO drastically

reduces communication costs.

3) **MSB-known Optimization**: As pointed out by [16], [17], 2PC protocols can be more efficient when the MSB of the secret shares is known. Since the activation after ReLU is always non-negative, protocols including truncation and extension can be further optimized. In UFO, we locate the ReLU function and then, propagate the sign of the activations to all the downstream protocols. In Figure 10, for example, the input of ①②③ must be non-negative, so they can be optimized. In contrast, ④⑤ can not be optimized since the GEMM outputs can be either positive or negative.

C. Complexity and Formal Description of Protocol Fusion

1) **Complexity Analysis**: The communication complexity per element mainly scales with the initial bit width l_1 . Also, for a given matrix with the dimension of $d_1 \times d_1 \times d_3$, the number of extensions needed would be $d_1 \times d_1 \times d_3$. Therefore, the total communication complexity of extension for a matrix becomes $O(d_1 d_2 d_3 (\lambda(l_1 + 1) + 13l_1 + l_2))$. In Figure 10, the extension communication of feature extension (block ②) is $O(HWC(\lambda(l_1 + 1) + 13l_1 + l_2))$ while that of output extension (block ⑤) is $O(KT(m+r-1)^2(\lambda(l_1 + 1) + 13l_1 + l_2))$, which is more expensive.

2) **Protocol Fusion**: We provide the following propositions to elaborate the principle of protocol fusion.

Proposition 1: For a given $\langle x \rangle^{(l_1)}$, $\Pi_{\text{Trunc}}^{l_1, l_2}(\langle x \rangle^{(l_1)})$ can be decomposed into $\Pi_{\text{TR}}^{l_1, l_2}$ followed by $\Pi_{\text{Ext}}^{l_1 - l_2, l_1}$ as

$$\Pi_{\text{Trunc}}^{l_1, l_2}(\langle x \rangle^{(l_1)}) = \Pi_{\text{Ext}}^{l_1 - l_2, l_1}(\Pi_{\text{TR}}^{l_1, l_2}(\langle x \rangle^{(l_1)})).$$

The decomposition does not change communication.

Proposition 2: If a given $\langle x \rangle^{(l_1)}$ is extended to l_2 -bit first and then extended to l_3 -bit. Then, the two neighboring extensions can be fused together as

$$\Pi_{\text{Ext}}^{l_2, l_3}(\Pi_{\text{Ext}}^{l_1, l_2}(\langle x \rangle^{(l_1)})) = \Pi_{\text{Ext}}^{l_1, l_3}(\langle x \rangle^{(l_1)}).$$

Extension fusion reduces communication from $O(\lambda(l_1 + l_2 + 2))$ to $O(\lambda(l_1 + 1))$.

Proposition 3: For a given $\langle x \rangle^{(l_1)}$, when re-quantization ends up with truncation, and is followed by an extension, the protocol can be first decomposed and then fused as

$$\begin{aligned} & \Pi_{\text{Ext}}^{l_1, l_3}(\Pi_{\text{Trunc}}^{l_1, l_2}(\langle x \rangle^{(l_1)})) \\ &= \Pi_{\text{Ext}}^{l_1, l_3}(\Pi_{\text{Ext}}^{l_1 - l_2, l_1}(\Pi_{\text{TR}}^{l_1, l_2}(\langle x \rangle^{(l_1)}))) \\ &= \Pi_{\text{Ext}}^{l_1 - l_2, l_3}(\Pi_{\text{TR}}^{l_1, l_2}(\langle x \rangle^{(l_1)})). \end{aligned}$$

Combining Proposition 1 and 2, this fusion reduces communication by around $2\times$ from $O(\lambda(2l_1 + 4))$ to $O(\lambda(l_1 + 2))$.

D. Security and Correctness Analysis of UFO

UFO is built on top of SiRNN [2] with a new quantized Winograd convolution protocol and graph-level protocol optimizations. The security of the QWinConv protocol directly follows the security guarantee from OT primitive [30]. Observe that all the communication between the client and the server is

performed through OT which ensures the privacy of both the selection bits and messages. Graph-level protocol optimizations leverage information known to both parties, e.g., the model architecture, and thus, do not reveal extra information. Utilizing quantized neural networks does not affect OT primitives in any way. The correctness of the QWinConv protocol is guaranteed by the theorem of Winograd transformation [34] and we use bit extensions to avoid inference errors.

V. QUANTIZATION ALGORITHM OPTIMIZATION

In this section, we propose a Winograd-domain QAT algorithm that is compatible with OT-based 2PC inference. The training procedure is shown in Algorithm 1. We first assign layer-wise bit widths based on quantization sensitivity (line 2) and then propose 2PC-friendly bit re-weighting to consider weight outliers (line 3-8). Then, training is performed (line 9-14). We demonstrate where to insert the quantization operation in Figure 3. Then, 2PC inference based on optimized protocols and re-weighted bit importance is performed in Algorithm 2.

A. 2PC-aware Sensitivity-based Bit Width Assignment

Different layers in a CNN have different sensitivity to the quantization noise [43]–[45]. To enable accurate and efficient private inference of UFO, we propose a 2PC-aware mixed-precision algorithm to search for the optimal bit width for each layer based on sensitivity. Following HAWQ [43]–[45], sensitivity can be approximately measured by the average trace of the Hessian matrix, and layers with a larger trace of the Hessian matrix are more sensitive to quantization. Let Ω_i denote the output perturbation induced by quantizing the i -th layer. Then, we have

$$\Omega_i = \overline{\text{Tr}}(H_i) \cdot \|\mathbb{Q}(GW_i G^\top) - GW_i G^\top\|_2^2,$$

where H_i and $\overline{\text{Tr}}(H_i)$ denote the Hessian matrix and average trace, $\|\mathbb{Q}(GW_i G^\top) - GW_i G^\top\|_2^2$ denotes the L_2 norm of Winograd quantization perturbation. Now we consider the factor of 2PC communication cost. Given the communication bound ζ and an L -layer model, we formulate the 2PC-aware bit width assignment problem as an integer linear programming problem (ILP) as

$$\min_{\{b_i\}_{i=1}^L} \sum_{i=1}^L \Omega_i^{b_i}, \quad \text{s.t.} \quad \sum_{i=1}^L C_i^{b_i} \leq \zeta,$$

where $C_i^{b_i}$ is the associated communication cost and $\Omega_i^{b_i}$ is perturbation when quantizing the i -th layer to b_i -bit. The objective is to find the optimal bit width assignment $\{b_i\}_{i=1}^L$ to minimize the perturbation of the model output under the given communication constraint.

B. 2PC-friendly Bit Re-weighting Algorithm for Outliers

1) **Bit Re-weighting**: Based on the above algorithm, we assign the bit width of each layer. However, as mentioned in Section III, weight outliers introduced by Winograd transformations make quantization challenging, leading to inferior model accuracy. For OT-based linear layers, each weight is first written as $\sum_{b=0}^{l_w-1} w^{(b)} \cdot 2^b$ and then, each bit $w^{(b)}$ is

Algorithm 1: Training Procedure of UFO Quantization with Mixed Precision

Input : Pre-trained floating-point weights w_f , communication bound ζ , the number of layers L , finetuning epochs E .

Output: Set of bit importance \mathbb{B} and quantized weights w .

```

1 // Layer-wise bit width assignment (Sec. V-A)
2  $l_w = \text{HessianAlgorithm}(w_f, \zeta)$ ;
3 for  $i \in [1, \dots, L]$  do
4   // Original bit importance
5    $\mathbb{B}_i \leftarrow \{2^{l_{wi-1}}, 2^{l_{wi-2}}, \dots, 2^1, 2^0\}$ ;
6   if  $\text{HasOutliers}(w_i)$  then
7     // Bit re-weighting (Sec. V-B1)
8      $\mathbb{B}_i \leftarrow \{2^{l_{wi}}, 2^{l_{wi-2}}, \dots, 2^1, 2^0\}$ ;
9 for  $e \in [1, \dots, E]$  do
10  // Training (Sec. V-B2)
11  Forward propagation based on Equation (2);
12  Compute loss  $\mathcal{L}_{CE}$ ;
13  Back propagation based on Equation (3);
14  Update  $w$  with SGD optimizer;
15 return  $w$  and  $\mathbb{B}$ .
```

multiplied with the corresponding activations with a single OT. This provides us with opportunities to re-weight each bit by adjusting 2^b to increase the representation range without explicitly increasing the bit width or causing extra communication overhead. We define 2^b as the bit importance for b -th bit and define the set of 2^b as $\mathbb{B} = \{2^{l_w-1}, 2^{l_w-2}, \dots, 2^1, 2^0\}$. Then, the weight can be re-written as $\sum_{b=0}^{l_w-1} w^{(b)} \cdot \mathbb{B}[b]$. We first perform a one-time inference to check whether there are outliers in each layer based on the z-score. Then, for the layers with outliers, we re-weight the bit importance by adjusting 2^b to $2^{b'}$ where $b' > b$ to increase the representation range flexibly. In practice, we increase MSB by adjusting \mathbb{B} to $\{2^{l_w}, 2^{l_w-2}, \dots, 2^1, 2^0\}$ to accommodate the outliers.

2) **Finetuning:** After the bit re-weighting, we use QAT to finetune the quantized models. Since the bit importance is adjusted, we find it convenient to utilize the bit-level quantization strategy [46] for finetuning, which considers each bit $w^{(b)}$ as a separate trainable parameter. Specifically, the quantized weight after bit re-weighting can be formulated as

$$\text{Forward: } w_q = \frac{s \cdot \text{Round}(\sum_{b=0}^{l_w-1} w^{(b)} \cdot \mathbb{B}[b])}{2^{l_w-1}}, \quad (2)$$

$$\text{Backward: } \frac{\partial \mathcal{L}}{\partial w^{(b)}} = \frac{2^b}{2^{l_w-1}} \frac{\partial \mathcal{L}_{CE}(\mathcal{M}_{w_q}(x), y)}{\partial w_q}, \quad (3)$$

where (x, y) denotes input-label pair, s denotes the scaling factor, \mathcal{L}_{CE} denotes cross-entropy loss, \mathcal{M}_{w_q} denotes the model with quantized weight w_q . During finetuning, both $w^{(b)}$ and s are trainable via STE [47].

3) **Inference:** After finetuning, we obtain each layer's quantized weights and the adjusted bit importance \mathbb{B} . The

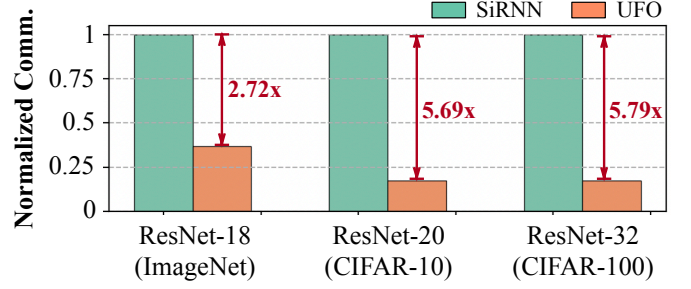


Fig. 13: Micro-benchmark of residual protocol.

inference pipeline is shown in Algorithm 2. For the i -th layer, QWinConv represents weight as $w_i = \sum_{b=0}^{l_w-1} w_i^{(b)} \cdot \mathbb{B}_i[b]$, and each bit $w_i^{(b)}$ is multiplied with the activation with OT. The final results are acquired by combining the partial results by shift and addition. Residual protocol follows Section IV-B2.

VI. EXPERIMENTAL RESULTS

A. Experimental Setups

1) **Inference Framework:** UFO is implemented on the top of SiRNN [2] in EzPC² library in C++ for private inference. Specifically, our quantized Winograd convolution is implemented in C++ with Eigen and Armadillo libraries. Following [1], [16], we use LAN mode for communication, where the bandwidth is 377 MBps and echo latency is 0.3ms. In our experiments, we evaluate the inference efficiency on the Intel Xeon Gold 5220R CPU @ 2.20GHz.

2) **Models and Datasets:** We conduct experiments on various models and datasets, i.e., MiniONN [5] and ResNet-20 on CIFAR-10, ResNet-32 on CIFAR-100, ResNet-18 on Tiny-ImageNet and ImageNet [48]. Baseline DeepReDuce [49], SNL [14], SAFENet [50], and SENet [15] are ReLU-reduced methods evaluated using SiRNN.

3) **QAT Details:** To improve the performance of quantized models, we adopt quantization-aware training with the PyTorch framework for Winograd-based models. During training, we fix the transformation matrices A, B while G is set to be trainable since GWG^T is computed and quantized offline. For MiniONN, we fix the bit width of activation to 4-bit while for ResNets, we fix it to 6-bit, and we only search the bit widths for weights. We always use high precision, i.e., 8 bits, for the residual for better accuracy [27], [41], [42].

B. Micro-benchmark Evaluation

1) **Convolution Protocol:** To verify the effectiveness of our proposed QWinConv protocol, we benchmark the convolution communication in Table IV. We compare UFO with SiRNN [2] and CoPriv [11] given different layer dimensions. As observed, with W2A4, UFO achieves 15.8~24.8 \times and 9.6~14.7 \times communication reduction, compared to SiRNN and CoPriv, respectively.

²<https://github.com/mpc-msri/EzPC>

Algorithm 2: Detailed 2PC Inference Protocol of UFO for a Single ResNet Block

Input : Secret-shared input $\langle \mathbf{X} \rangle \in \mathbb{Z}_{2^{l_{in}}}^{N \times C \times H \times W}$, quantized weights \mathbf{W} , Winograd transformation matrices $\mathbf{A}, \mathbf{B}, \mathbf{G}$.

Output: Secret-shared output $\langle \mathbf{Y} \rangle \in \mathbb{Z}_{2^{l_{out}}}^{N \times K \times H' \times W'}$.

1 [Offline Phase] Weight Transformation and Quantization

```

2    $\mathbf{W}_{win} \leftarrow \mathbf{G}\mathbf{W}\mathbf{G}^T$ ; // Weight transformation (Eq. (1))
3    $\mathbf{W}_q \leftarrow \text{Quant}(\mathbf{W}_{win})$ ; // Weight quantization with bit re-weighting (Sec. V)

```

4 [Online Phase] Winograd-based Convolution, Non-linear Layer, Residual

```

5   // ===== Quantized Winograd Convolution =====
6   // 1. Feature Partitioning
7    $\langle \tilde{\mathbf{X}} \rangle \leftarrow \text{Partition}(\langle \mathbf{X} \rangle)$ 
8   // 2. Feature Transformation (Local Computation)
9    $\langle \tilde{\mathbf{X}} \rangle_{ext} \leftarrow \Pi_{\text{Ext}}(\langle \tilde{\mathbf{X}} \rangle)$ ; // Extend bit width to prevent overflow
10   $\langle \mathbf{U} \rangle \leftarrow \mathbf{B}^T \langle \tilde{\mathbf{X}} \rangle_{ext} \mathbf{B}$ ; // Computed locally on each tile (Eq. (1))
11  // 3. Winograd-domain GEMM
12   $\langle \mathbf{M} \rangle \leftarrow \Pi_{\text{GEMM}}(\mathbf{W}_q^{(l)}, \langle \mathbf{U} \rangle)$ ; // OT-based GEMM with communication (Eq. (1))
13  // 4. Output Transformation (Local Computation)
14   $\langle \mathbf{M} \rangle_{ext} \leftarrow \Pi_{\text{Ext}}(\langle \mathbf{M} \rangle)$ ; // Extend bit width to prevent overflow
15   $\langle \mathbf{Y} \rangle \leftarrow \mathbf{A}^T \langle \mathbf{M} \rangle_{ext} \mathbf{A}$ ; // Computed locally on each tile (Eq. (1))
16  // ===== Non-Linear Layer =====
17   $\langle \mathbf{Y} \rangle \leftarrow \text{ReLU}(\langle \mathbf{Y} \rangle)$ ; // MSB-known optimization (Sec. IV-B3)
18   $\langle \mathbf{Y} \rangle \leftarrow \Pi_{\text{Trunc}}(\langle \mathbf{Y} \rangle)$ ; // Re-quantize to  $l_{in}$ 
19  // ===== Quantized Winograd Convolution =====
20  Repeat step # 5–15 with  $\langle \mathbf{Y} \rangle$  as the input to obtain the output  $\langle \mathbf{Y}_{out} \rangle$ ;
21  // ===== Simplified Residual Protocol =====
22   $\langle \mathbf{X} \rangle_{ext} \leftarrow \Pi_{\text{Ext}}(\langle \mathbf{X} \rangle)$ ; // Align output bit width and scale
23   $\langle \mathbf{Y} \rangle \leftarrow \langle \mathbf{Y}_{out} \rangle + \langle \mathbf{X} \rangle_{ext}$ ; // Addition for residual (IV-B2)
24  return  $\langle \mathbf{Y} \rangle$ ;

```

TABLE IV: Micro-benchmark (MB) of convolution protocol.

Height	Width	#Input Channel	#Output Channel	SiRNN	CoPriv	UFO (W2A4)	UFO (W2A6)
32	32	16	32	414.1	247.3	25.75	30.88
16	16	32	64	380.1	247.3	17.77	20.33
56	56	64	64	9336	5554	376.9	440.6
28	28	128	128	8598	5491	381.9	438.9

2) **Residual Protocol**: In Figure 13, we compare our simplified residual protocol with SiRNN. We focus on the comparison with SiRNN as other works usually ignore the protocol and suffer from computation errors. UFO achieves 2.7 \times , 5.7 \times and 5.8 \times communication reduction on ResNet-18, ResNet-20, and ResNet-32, respectively.

C. End-to-end Inference Evaluation

1) **CIFAR-10 and CIFAR-100**: From Figure 14, we make the following observations: 1) UFO achieves state-of-the-art Pareto front of the accuracy and efficiency. Specifically, on CIFAR-10, UFO outperforms SiRNN with 0.71% higher accuracy and 9.41 \times communication reduction. On CIFAR-100, UFO achieves 1.29% higher accuracy with 11.7 \times and 6.33 \times communication reduction compared with SiRNN and CoPriv, respectively; 2) compared with COINN, UFO achieves 1.4% and 1.16% higher accuracy with 2.1 \times and 3.6 \times communication reduction on CIFAR-10 and CIFAR-100, respectively;

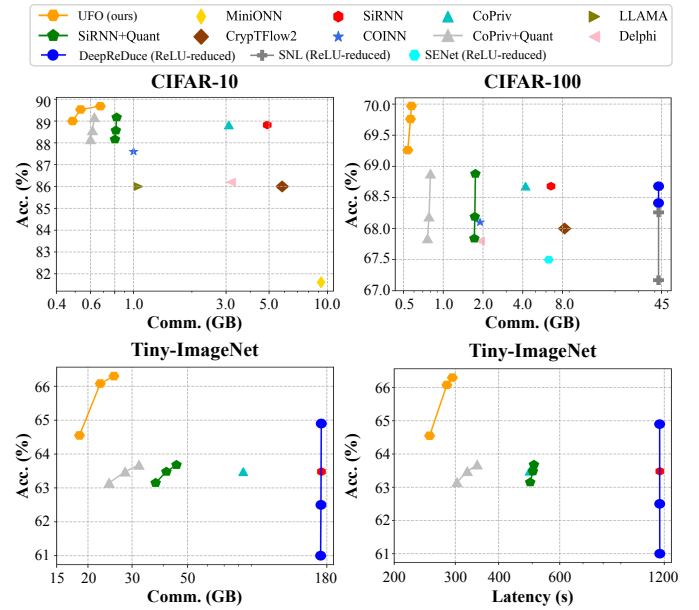


Fig. 14: End-to-end comparison with prior-art methods.

3) when compared with ReLU-reduced methods, including DeepReDuce [8], SAFENet [50] and SNL [14]. The result shows these methods cannot effectively reduce total communication, and UFO achieves more than 80 \times and 15 \times

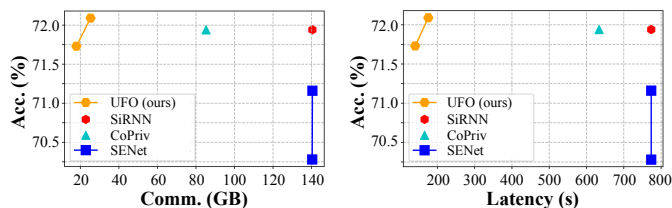


Fig. 15: Evaluation on ImageNet.

TABLE V: Comparison with prior-art Winograd quantization methods on CIFAR-10.

Method	Comm. (GB)	Lat. (s)	Top-1 Acc. (%)
PTQ [51]	0.783	56.85	80.63
Legendre [35]	0.965	61.86	91.80
BQW [36]	0.783	56.16	90.74
PAW [37]	0.784	57.01	90.25
WinoVidiVici [38]	0.964	60.40	92.29
UFO (ours)	0.366	13.82	92.57

communication reduction with higher accuracy, compared with DeepReDuce/SNL and SAFENet, respectively.

2) *Tiny-ImageNet and ImageNet*: We compare UFO with SiRNN, CoPriv, and ReLU-optimized method DeepReDuce on Tiny-ImageNet. As shown in Figure 14, we observe that 1) UFO achieves $9.26\times$ communication reduction with 1.07% higher accuracy compared with SiRNN; 2) compared with SiRNN with mixed-precision, UFO achieves $2.44\times$ communication reduction and 0.87% higher accuracy; 3) compared with CoPriv, UFO achieves $4.5\times$ communication reduction with 1.07% higher accuracy. We also evaluate the accuracy and efficiency of UFO on ImageNet in Figure 15, UFO achieves $4.88\times$ and $2.96\times$ communication reduction with 0.15% higher accuracy compared with SiRNN and CoPriv, respectively.

D. Comparison with Prior-art Winograd Quantization

We compare UFO with prior-art Winograd quantization algorithms, including Legendre [35], BQW [36], and PAW [37] on ResNet-20 and CIFAR-10. In Table V, UFO consistently achieves higher accuracy and higher inference efficiency, demonstrating the effectiveness of our quantization algorithm. For example, compared to WinoVidiVici [38], UFO achieves $2.63\times$ communication and $4.37\times$ latency reduction, respectively with 0.28% higher accuracy.

E. Comparison with HE-based Frameworks

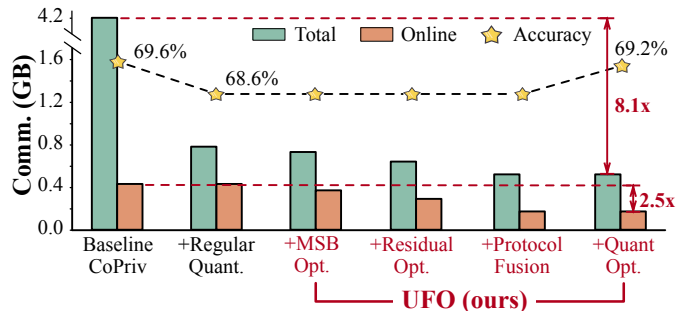
We also compare UFO with representative HE-based methods Gazelle [22], Delphi [4], CryptFlow2 [1] on CIFAR-100 in Table VI, and UFO achieves significantly higher efficiency and accuracy. For example, compared to CryptFlow2 [1], UFO achieves $1.30\times$ and $4.87\times$ communication and latency reduction, respectively. Additionally, the proposed UFO can be generally applied to HE-based frameworks and protocols, which we leave to our future work.

F. Ablation Studies

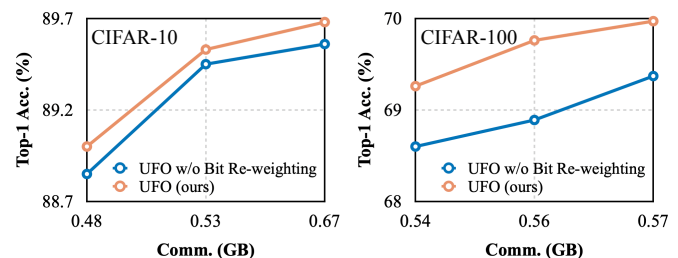
1) *Effectiveness of Different Optimizations*: To understand how different optimizations help improve 2PC inference, we

TABLE VI: End-to-end comparison with HE-based methods.

Method	Comm. (GB)	Lat. (s)	Top-1 Acc. (%)
Gazelle [22]	8.900	238.7	67.90
Delphi [4]	6.500	200.0	67.80
CryptFlow2 [1] ¹	0.681	99.03	68.00
UFO (ours)	0.525	20.33	69.26

¹ Use the version that linear layers are implemented using HE protocol.

(a) Ablation Study of Different Optimizations



(b) Ablation Study of Quantization Strategy

Fig. 16: Effectiveness of our proposed optimizations.

add the optimizations step by step on ResNet-32 and present the results in Figure 16. As observed from the results, we find that 1) low-precision quantization benefits the total communication efficiency most but there is no benefit for online communication due to the extra bit width conversions introduced from Winograd transformations; 2) protocol optimizations including the simplified residual protocol, protocol fusion, and MSB-known optimization consistently reduce the online and total communication, 3) although naively combining Winograd convolution with quantized private inference enlarges the online communication, our optimizations jointly achieve $8.1\times$ and $2.5\times$ total and online communication reduction, respectively, compared to CoPriv; 4) bit re-weighting improves the accuracy without sacrificing efficiency. The findings indicate all of our optimizations are indispensable for 2PC inference.

2) *Block-wise Visualization*: We show the block-wise communication comparison on ResNet-32 as shown in Figure 17. As observed, with our quantized Winograd convolution protocol, UFO achieves 63% communication reduction on average, and protocol fusion further reduces 30% communication. The results demonstrate the effectiveness of UFO and different layers benefit from UFO differently.

3) *Distribution of Bit Width Assignment*: We visualize the distribution of bit width assignment by the sensitivity-based method in Figure 18. As observed, the model tends to use lower bit widths in the middle layers rather than the initial and last layers. Meanwhile, a lower bit width allocation often

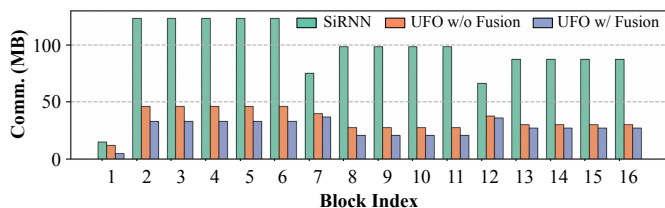


Fig. 17: Block-wise visualization of communication.

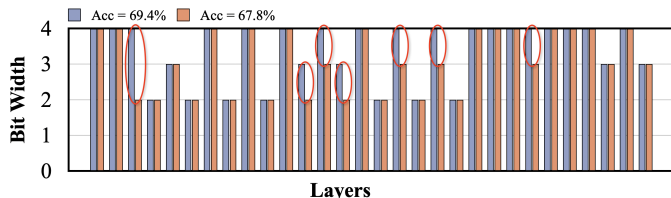


Fig. 18: Distribution of bit width assignment on ResNet-32.

corresponds to lower bit widths in the middle layers.

VII. RELATED WORK

There has been an increasing amount of literature on OT-based private inference, which can be generally categorized into the following three paradigms.

1) **Protocol Optimization**: A substantial body of work, such as CryptFlow2 [1], CryptTen [52], SecureML [3] leverage OT to evaluate both linear and non-linear layers. SiRNN [2] further extends the protocols to mixed bit widths, while Secfloat [53] extends the protocols to floating-point representation. Squirrel [9] builds new protocols to support gradient boosting decision tree (GBDT) training. CipherGPT [54] optimizes the GEMM using VOLE to significantly reduce communication overhead. Studies like [17], [19]–[21] use OT to evaluate the non-linear layers.

2) **Algorithm Optimization**: Many research efforts have been made to linear layer optimization [55], [56], ReLU and GeLU optimization [8], [14], [15], [57]–[59], and Softmax optimization [58], [60]–[62]. Classically, MPCFormer [61] replaces Softmax with MPC-friendly polynomial approximations. MPCViT [58] replaces the exponential in Softmax with ReLU and selectively uses linear attention using neural architecture search (NAS). CryptPEFT [63] confines expensive cryptographic operators within lightweight adapters and utilizes NAS to identify optimal adapter architecture.

3) **Co-optimization**: Besides optimizing the protocol and algorithm alone, Delphi [4] transfers most of the online cost to the offline phase and uses NAS to reduce ReLUs. COINN [13] proposes factorized GEMM by weight clustering and a corresponding protocol to reduce the number of multiplications. CoPriv [11] integrates the Winograd convolution protocol, ReLU pruning, and layer fusion to cut down the overall communication cost. PrivQuant [27] uses mixed-precision quantization with protocol fusion and MSB-known optimization to reduce the overhead.

Another line of work attempts to reduce inference overhead with quantization [2], [6], [13], [40], [64]–[66]. For instance, Ditto [66] adopts static dyadic quantization to avoid dynamically computing scale during inference and proposes

type conversion protocols for efficient bit width conversion. In Table III, we compare UFO with previous works qualitatively.

VIII. CONCLUSION AND FUTURE WORK

In this work, we propose UFO, an efficient 2PC-based framework seamlessly combining Winograd convolution and quantization. Based on the observation that naively combining quantization and Winograd is sub-optimal, we propose a series of protocol optimizations to minimize the communication and develop a mixed-precision QAT algorithm with a bit re-weighting algorithm to improve the accuracy and efficiently accommodate quantization outliers. Extensive experiments demonstrate that UFO consistently enhances the efficiency without compromising the accuracy compared with the prior-art baselines across a variety of protocols and algorithms.

This work utilizes the Winograd algorithm to optimize the convolution layers, which is tailored for CNNs. Given that Winograd-based acceleration does not directly translate to Transformer-based architectures, the scope of this paper is focused on CNNs. Extending our methodology to Transformers remains a promising direction for future research. Moreover, our future work also includes investigating Winograd optimizations with HE protocols. This necessitates specialized designs for HE-friendly encoding and quantization algorithms.

REFERENCES

- [1] D. Rathee, M. Rathee, N. Kumar, N. Chandran, D. Gupta, A. Rastogi, and R. Sharma, “Cryptflow2: Practical 2-party secure inference,” in *CCS*, 2020, pp. 325–342.
- [2] D. Rathee, M. Rathee, R. K. K. Goli, D. Gupta, R. Sharma, N. Chandran, and A. Rastogi, “SiRnn: A math library for secure rnn inference,” in *SP*. IEEE, 2021, pp. 1003–1020.
- [3] P. Mohassel and Y. Zhang, “Secureml: A system for scalable privacy-preserving machine learning,” in *SP*. IEEE, 2017, pp. 19–38.
- [4] P. Mishra, R. Lehmkuhl, A. Srinivasan, W. Zheng, and R. A. Popa, “Delphi: A cryptographic inference system for neural networks,” in *Proceedings of the 2020 Workshop on Privacy-Preserving Machine Learning in Practice*, 2020, pp. 27–30.
- [5] J. Liu, M. Juuti, Y. Lu, and N. Asokan, “Oblivious neural network predictions via minionn transformations,” in *CCS*, 2017, pp. 619–631.
- [6] L. Shen, Y. Dong, B. Fang, J. Shi, X. Wang, S. Pan, and R. Shi, “Abnn2: Secure two-party arbitrary-bitwidth quantized neural network predictions,” in *DAC*, 2022, pp. 361–366.
- [7] W. Zeng, T. Xu, Y. Chen, Y. Zhou, M. Zhang, J. Tan, C. Hong, and M. Li, “Towards efficient privacy-preserving machine learning: A systematic review from protocol, model, and system perspectives,” *arXiv preprint arXiv:2507.14519*, 2025.
- [8] N. K. Jha, Z. Ghodsi, S. Garg, and B. Reagen, “Deepreduce: Relu reduction for fast private inference,” in *ICML*. PMLR, 2021, pp. 4839–4849.
- [9] W. jie Lu, Z. Huang, Q. Zhang, Y. Wang, and C. Hong, “Squirrel: A scalable secure Two-Party computation framework for training gradient boosting decision tree,” in *USENIX Security*, Anaheim, CA, 2023, pp. 6435–6451.
- [10] P. Mohassel and P. Rindal, “Aby3: A mixed protocol framework for machine learning,” in *CCS*, 2018, pp. 35–52.
- [11] W. Zeng, M. Li, H. Yang, W. jie Lu, R. Wang, and R. Huang, “Copriv: Network/protocol co-optimization for communication-efficient private inference,” in *NeurIPS*, 2023.
- [12] M. S. Riazi, M. Samragh, H. Chen, K. Laine, K. Lauter, and F. Koushanfar, “{XONN}:{XNOR-based} oblivious deep neural network inference,” in *USENIX Security*, 2019, pp. 1501–1518.
- [13] S. U. Hussain, M. Javaheripi, M. Samragh, and F. Koushanfar, “Coinn: Crypto/ml codesign for oblivious inference via neural networks,” in *CCS*, 2021, pp. 3266–3281.
- [14] M. Cho, A. Joshi, B. Reagen, S. Garg, and C. Hegde, “Selective network linearization for efficient private inference,” in *ICML*. PMLR, 2022, pp. 3947–3961.

- [15] S. Kundu, S. Lu, Y. Zhang, J. Liu, and P. A. Beeren, "Learning to linearize deep neural networks for secure and efficient private inference," *arXiv preprint arXiv:2301.09254*, 2023.
- [16] Z. Huang, W.-j. Lu, C. Hong, and J. Ding, "Cheetah: Lean and fast secure {two-party} deep neural network inference," in *USENIX Security*, 2022, pp. 809–826.
- [17] M. Hao, H. Li, H. Chen, P. Xing, G. Xu, and T. Zhang, "Iron: Private inference on transformers," *NeurIPS*, vol. 35, pp. 15 718–15 731, 2022.
- [18] T. Xu, M. Li, R. Wang, and R. Huang, "Falcon: Accelerating homomorphically encrypted convolutions for efficient private mobile network inference," in *ICCAD*. IEEE, 2023, pp. 1–9.
- [19] Q. Pang, J. Zhu, H. Möllering, W. Zheng, and T. Schneider, "Bolt: Privacy-preserving, accurate and efficient inference for transformers," *Cryptology ePrint Archive*, 2023.
- [20] W.-j. Lu, Z. Huang, Z. Gu, J. Li, J. Liu, C. Hong, K. Ren, T. Wei, and W. Chen, "Bumblebee: Secure two-party inference framework for large transformers," *Cryptology ePrint Archive*, 2023.
- [21] T. Xu, W.-j. Lu, J. Yu, Y. Chen, C. Lin, R. Wang, and M. Li, "Breaking the layer barrier: Remodeling private transformer inference with hybrid {CKKS} and {MPC}," in *USENIX Security*, 2025, pp. 2653–2672.
- [22] C. Juvekar, V. Vaikuntanathan, and A. Chandrakasan, "{GAZELLE}: A low latency framework for secure neural network inference," in *USENIX Security*, 2018, pp. 1651–1669.
- [23] J. He, K. Yang, G. Tang, Z. Huang, L. Lin, C. Wei, Y. Yan, and W. Wang, "Rhombus: Fast homomorphic matrix-vector multiplication for secure two-party inference," in *CCS*, 2024, pp. 2490–2504.
- [24] J. H. Ju, J. Park, J. Kim, M. Kang, D. Kim, J. H. Cheon, and J. H. Ahn, "Neujeans: Private neural network inference with joint optimization of convolution and the bootstrapping," in *CCS*, 2024, pp. 4361–4375.
- [25] J. Moon, D. Yoo, X. Jiang, and M. Kim, "Thor: Secure transformer inference with homomorphic encryption," in *CCS*, 2025, pp. 3765–3779.
- [26] J. Yu, W. Zeng, T. Xu, R. Chen, Y. Liang, R. Wang, R. Huang, and M. Li, "Flexhe: A flexible kernel generation framework for homomorphic encryption-based private inference," in *ICCAD*, 2024, pp. 1–9.
- [27] T. Xu, S. Zhong, W. Zeng, R. Wang, and M. Li, "Privquant: Communication-efficient private inference with quantized network/protocol co-optimization," *arXiv preprint arXiv:2410.09531*, 2024.
- [28] J. Fan and F. Vercauteren, "Somewhat practical fully homomorphic encryption," *Cryptology ePrint Archive*, 2012.
- [29] T. Xu, M. Li, and R. Wang, "Hequant: Marrying homomorphic encryption and quantization for communication-efficient private inference," *arXiv preprint arXiv:2401.15970*, 2024.
- [30] M. Naor and B. Pinkas, "Efficient oblivious transfer protocols," in *SODA*, vol. 1, 2001, pp. 448–457.
- [31] R. Krishnamoorthi, "Quantizing deep convolutional networks for efficient inference: A whitepaper," *arXiv preprint arXiv:1806.08342*, 2018.
- [32] Y. Lin, H. Tang, S. Yang, Z. Zhang, G. Xiao, C. Gan, and S. Han, "Qserve: W4a8kv4 quantization and system co-design for efficient llm serving," *Proceedings of Machine Learning and Systems*, vol. 7, 2025.
- [33] R. Wei, S. Xu, L. Zhong, Z. Yang, Q. Guo, Y. Wang, R. Wang, and M. Li, "Lightmamba: Efficient mamba acceleration on fpga with quantization and hardware co-design," in *DATe*. IEEE, 2025, pp. 1–7.
- [34] A. Lavin and S. Gray, "Fast algorithms for convolutional neural networks," in *CVPR*, 2016, pp. 4013–4021.
- [35] B. Barabasz, "Quantized winograd/toom-cook convolution for dnns: Beyond canonical polynomials base," *arXiv preprint arXiv:2004.11077*, 2020.
- [36] V. Chikin and V. Kryzhanovskiy, "Channel balancing for accurate quantization of winograd convolutions," in *CVPR*, 2022, pp. 12 507–12 516.
- [37] T. Chen, W. Xu, W. Chen, P. Wang, and J. Cheng, "Towards efficient and accurate winograd convolution via full quantization," *NeurIPS*, vol. 36, 2024.
- [38] P. Mori, L. Frickenstein, S. B. Sampath, M. Thoma, N. Fafous, M. R. Vemparala, A. Frickenstein, C. Unger, W. Stechele, D. Mueller-Gritschneider *et al.*, "Wino vidi vici: Conquering numerical instability of 8-bit winograd convolution for accurate inference acceleration on edge," in *WACV*, 2024, pp. 53–62.
- [39] S. Pan, G. Tuzi, S. Sreeram, and D. Gope, "Data-free group-wise fully quantized winograd convolution via learnable scales," in *Proceedings of the Computer Vision and Pattern Recognition Conference*, 2025, pp. 4091–4100.
- [40] N. Agrawal, A. Shahin Shamsabadi, M. J. Kusner, and A. Gascón, "Quotient: two-party secure neural network training and prediction," in *CCS*, 2019, pp. 1231–1247.
- [41] L. Yang and Q. Jin, "Fracbits: Mixed precision quantization via fractional bit-widths," in *AAAI*, vol. 35, no. 12, 2021, pp. 10 612–10 620.
- [42] B. Wu, Y. Wang, P. Zhang, Y. Tian, P. Vajda, and K. Keutzer, "Mixed precision quantization of convnets via differentiable neural architecture search," *arXiv preprint arXiv:1812.00090*, 2018.
- [43] Z. Dong, Z. Yao, A. Gholami, M. W. Mahoney, and K. Keutzer, "Hawq: Hessian aware quantization of neural networks with mixed-precision," in *ICCV*, 2019, pp. 293–302.
- [44] Z. Dong, Z. Yao, D. Arfeen, A. Gholami, M. W. Mahoney, and K. Keutzer, "Hawq-v2: Hessian aware trace-weighted quantization of neural networks," *NeurIPS*, vol. 33, pp. 18 518–18 529, 2020.
- [45] Z. Yao, Z. Dong, Z. Zheng, A. Gholami, J. Yu, E. Tan, L. Wang, Q. Huang, Y. Wang, M. Mahoney *et al.*, "Hawq-v3: Dyadic neural network quantization," in *ICML*. PMLR, 2021, pp. 11 875–11 886.
- [46] H. Yang, L. Duan, Y. Chen, and H. Li, "Bsq: Exploring bit-level sparsity for mixed-precision neural network quantization," *arXiv preprint arXiv:2102.10462*, 2021.
- [47] Y. Bengio, N. Léonard, and A. Courville, "Estimating or propagating gradients through stochastic neurons for conditional computation," *arXiv preprint arXiv:1308.3432*, 2013.
- [48] J. Deng, W. Dong, R. Socher, L.-J. Li, K. Li, and L. Fei-Fei, "Imagenet: A large-scale hierarchical image database," in *CVPR*. Ieee, 2009, pp. 248–255.
- [49] N. K. Jha and B. Reagen, "Deepreshape: Redesigning neural networks for efficient private inference," *arXiv preprint arXiv:2304.10593*, 2023.
- [50] Q. Lou, Y. Shen, H. Jin, and L. Jiang, "Safenet: A secure, accurate and fast neural network inference," in *ICLR*, 2020.
- [51] Y. Li, R. Gong, X. Tan, Y. Yang, P. Hu, Q. Zhang, F. Yu, W. Wang, and S. Gu, "Breq: Pushing the limit of post-training quantization by block reconstruction," *arXiv preprint arXiv:2102.05426*, 2021.
- [52] B. Knott, S. Venkataraman, A. Hannun, S. Sengupta, M. Ibrahim, and L. van der Maaten, "Crypten: Secure multi-party computation meets machine learning," *NeurIPS*, vol. 34, pp. 4961–4973, 2021.
- [53] D. Rathee, A. Bhattacharya, R. Sharma, D. Gupta, N. Chandran, and A. Rastogi, "Secfloat: Accurate floating-point meets secure 2-party computation," in *2022 IEEE Symposium on Security and Privacy (SP)*. IEEE, 2022, pp. 576–595.
- [54] X. Hou, J. Liu, J. Li, Y. Li, W.-j. Lu, C. Hong, and K. Ren, "Ciphergpt: Secure two-party gpt inference," *Cryptology ePrint Archive*, 2023.
- [55] V. Ganesan, A. Bhattacharya, P. Kumar, D. Gupta, R. Sharma, and N. Chandran, "Efficient ml models for practical secure inference," *arXiv preprint arXiv:2209.00411*, 2022.
- [56] Y. Cai, Q. Zhang, R. Ning, C. Xin, and H. Wu, "Hunter: He-friendly structured pruning for efficient privacy-preserving deep learning," in *Proceedings of the 2022 ACM on Asia Conference on Computer and Communications Security*, 2022, pp. 931–945.
- [57] H. Peng, S. Huang, T. Zhou, Y. Luo, C. Wang, Z. Wang, J. Zhao, X. Xie, A. Li, T. Geng *et al.*, "Autorep: Automatic relu replacement for fast private network inference," in *ICCV*, 2023, pp. 5178–5188.
- [58] W. Zeng, M. Li, W. Xiong, T. Tong, W.-j. Lu, J. Tan, R. Wang, and R. Huang, "Mpcvit: Searching for accurate and efficient mpc-friendly vision transformer with heterogeneous attention," in *ICCV*, 2023, pp. 5052–5063.
- [59] F. Li, Y. Zhai, S. Cai, and M. Gao, "Seesaw: Compensating for nonlinear reduction with linear computations for private inference," in *Forty-first International Conference on Machine Learning*, 2024.
- [60] W. Zeng, Y. Dong, J. Zhou, J. Ma, J. Tan, R. Wang, and M. Li, "Mpcache: Mpc-friendly kv cache eviction for efficient private large language model inference," *arXiv preprint arXiv:2501.06807*, 2025.
- [61] D. Li, R. Shao, H. Wang, H. Guo, E. P. Xing, and H. Zhang, "Mpc-former: fast, performant and private transformer inference with mpc," *arXiv preprint arXiv:2211.01452*, 2022.
- [62] N. Dhyani, J. Mo, M. Cho, A. Joshi, S. Garg, B. Reagen, and C. Hegde, "Privit: Vision transformers for fast private inference," *arXiv preprint arXiv:2310.04604*, 2023.
- [63] S. Xia, W. Wang, Z. Wang, Y. Zhang, Y. Jin, D. Meng, and R. Hou, "Cryptpft: Efficient and private neural network inference via parameter-efficient fine-tuning," *arXiv preprint arXiv:2508.12264*, 2025.
- [64] M. Samragh, S. Hussain, X. Zhang, K. Huang, and F. Koushanfar, "On the application of binary neural networks in oblivious inference," in *CVPR*, 2021, pp. 4630–4639.
- [65] S. Hasler, T. Krips, R. Küsters, P. Reiser, and M. Rivinius, "Overdrive lowgear 2.0: Reduced-bandwidth mpc without sacrifice," *Cryptology ePrint Archive*, 2023.
- [66] H. Wu, W. Fang, Y. Zheng, J. Ma, J. Tan, Y. Wang, and L. Wang, "Ditto: Quantization-aware secure inference of transformers upon mpc," *arXiv preprint arXiv:2405.05525*, 2024.